Developmental Biology 450 (2019) 82–89

Contents lists available at ScienceDirect

Developmental Biology

journal homepage: www.elsevier.com/locate/developmentalbiology

Short Communication

Differential contribution of the two waves of cardiac progenitors and their derivatives to aorta and pulmonary artery

Hengwei Jin [1], Huijuan Wang [1], Jie Li, Shan Yu, Mingjie Xu, Zhiqian Qiu, Meng Xia, Jingai Zhu, Qiuting Feng, Jun Xie, Biao Xu, Zhongzhou Yang [*]

State Key Laboratory of Pharmaceutical Biotechnology, Department of Cardiology, Nanjing Drum Tower Hospital, The Affiliated Hospital of Nanjing University Medical School and MOE Key Laboratory of Model Animal for Disease Study, Model Animal Research Center, Nanjing University, Nanjing 210061, China

ARTICLE INFO

Keywords:
Outflow tract
Aorta
Pulmonary artery
Cardiac progenitors
PDK1
Pulmonary stenosis

ABSTRACT

During mouse development, part of the cells derived from the second heart field (SHF) progenitors contributes to the elongation and enlargement of the outflow tract (OFT) that subsequently septates into the trunks of aorta (Ao) and pulmonary artery (PA). Thus, the cardiac progenitor-originated cells are distributed to both Ao and PA. Here, we investigated that how these cells are assigned to the two great arteries during OFT septation through lineage tracing technology. By use of the inducible *Mef2c-AHF-CreERT2; Rosa26*-mTmG reporter system, two waves of SHF progenitors and their derivatives were identified, and they made differential contribution to the Ao and PA, respectively. While the early wave of cells (at E7.5) was preferentially destined to the Ao, the second wave of cells (from E8.5 till E11.5) made its favorite path to the PA. In addition, we unveiled PDK1 as a critical regulator of the second wave of cells as deletion of *Pdk1* resulted in poorly developed PA leading to pulmonary stenosis. Thus, this study provides insights into the understanding of the pre-determined cell fate of the cardiac progenitor-derived cells with preferential contribution to the Ao and PA, as well as of the pathogenesis of pulmonary stenosis.

1. Introduction

Septation of the cardiac outflow tract (OFT) into the trunk of aorta (Ao) and pulmonary artery (PA) is critical for establishment of the systemic and pulmonary circulation in order to sustain normal physiology and survival (Kirby et al., 1983; Neeb et al., 2013; Plein et al., 2015; Van den Hoff et al., 1999). Abnormal OFT septation results in severe great arterial defects including persistent truncus arteriosus (PTA) and stenosis of Ao and PA, which profoundly compromises life quality (Dyer and Kirby, 2009; Fahed et al., 2013; Neeb et al., 2013).

Pulmonary stenosis (PS) is a common congenital heart defect (CHD) and occurs either as a component of complex CHD (such as Tetrology of Fallot, TOF) or as an isolated anomaly (Bruneau, 2008; Srivastava, 2006). Isolated PS accounts for approximately 5–10% of all CHDs (Zeigler, 2008). However, the causes for PS are still largely unknown but are believed strongly connective to improper development (Fahed et al., 2013).

During embryonic development, the cardiac progenitors from the second heart field (SHF) migrate into the OFT and differentiate into cardiomyocytes contributing to myocardium of both the OFT and the right ventricle (Buckingham et al., 2005; Francou et al., 2013; Meilhac et al., 2015; Waldo et al., 2005). Following OFT septation into the Ao and PA, the OFT cardiomyocytes derived from the SHF progenitors are assigned to the trunk of these two great arteries (Webb et al., 2003). Previous work from Margaret E. Buckingham and colleagues reported that the progenitors in a subdomain of the SHF, the anterior heart field (AHF) are prefigured into the myocardium at the base of prospective Ao and PA trunks (Bajolle et al., 2006, 2008). This study shed lights on understanding the formation of the two great arteries, and the etiology of CHDs affecting the arterial pole of the heart. Nonetheless, the identities of these progenitors and how they are prefigured are still elusive.

Here, we generated lineage-tracing mouse line to characterize the assignment of the SHF-derived cells into the trunk of Ao and PA during OFT septation. We have identified two waves of SHF progenitor-derived cells that made differential contribution to the Ao and PA, respectively. In addition, we have uncovered PDK1 as a critical regulator of the second wave of cells that preferentially contribute to the PA. Our study provides insights into the understanding of the pre-determined cell fate of the

* Corresponding author.
E-mail address: zhongzhouyang@nju.edu.cn (Z. Yang).
[1] Equal contribution.

https://doi.org/10.1016/j.ydbio.2019.03.019
Received 8 December 2018; Received in revised form 7 March 2019; Accepted 27 March 2019
Available online 2 April 2019

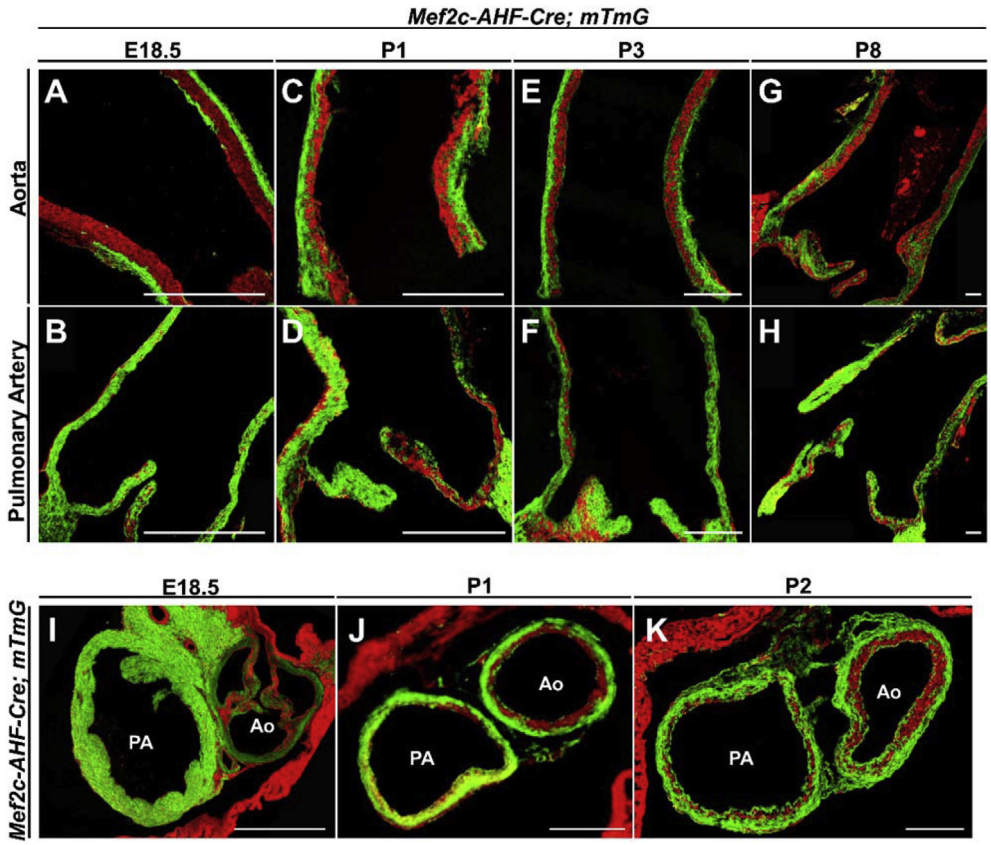

Fig. 1. Distinct contribution of the SHF-progenitor derived cells in the trunk of Ao and PA. **(A–H)** Lineage tracing of the *Mef2c-AHF* +cells (in green) in the trunks of the Ao and PA at E18.5, P1, P3 and P8 (longitudinal sections). **(I–K)** Lineage tracing of the *Mef2c-AHF* +cells (in green) in the trunks of the Ao and PA at E18.5, P1 and P2 (horizontal sections). Scale bars, 600 μm. Ao, aorta; PA, pulmonary artery.

cardiac progenitor-derived cells with preferential contribution to the Ao and PA, as well as of the pathogenesis of PS.

2. Results

2.1. Distinct contribution of the SHF-progenitor derived cells in the trunk of Ao and PA

The cardiac progenitors from the subdomain of the anterior heart field (AHF) in the second heart field (SHF) contribute to the development of the OFT and the right ventricle, and these cardiac progenitors possess the *Mef2c-AHF* enhancer activity (Verzi et al., 2005). Along with OFT septation, cells in the OFT wall are assigned to both Ao and PA. A previous study reported that the *Mef2c-AHF* +progenitor-derived cells populate the outer medial cells of the ascending aorta (Sawada et al., 2017). However, synchronic parallel study of these cells in both the Ao and PA is enormously lacking.

To simultaneously assess the contribution of the SHF progenitor-derived cells to both Ao and PA, we generated the *Mef2c-AHF-Cre; Rosa26*-mTmG (*Mef2c-AHF-Cre; mTmG*) mice and performed lineage tracing analysis using the *Mef2c-AHF* enhancer-driven reporter system to directly visualize the contribution of *Mef2c-AHF* +cells to these two great arteries. As shown in Fig. 1, GFP positive cells represented the *Mef2c-AHF* +cells while the RFP positive cells were non-*Mef2c-AHF*-derived cells. By the end of gestation at embryonic day 18.5 (E18.5), the base of the Ao trunk manifested ordered layers of cellular composition: the *Mef2c-AHF* +outer layer and the *Mef2c-AHF*- inner layer (Fig. 1A). In contrast, the PA trunk was consisted almost entirely of *Mef2c-AHF* +cells (Fig. 1B). We further analyzed these mice at postnatal ages of P1, P3 and P8 and similar patterns in the Ao and PA were largely maintained except that the boundary between *Mef2c-AHF*+and *Mef2c-AHF*- was less discernible in the Ao at P8 (Fig. 1C–H). As a complementary study to the longitudinal analysis, horizontal visualization of the cellular composition in the trunk of Ao and PA confirmed these patterns (Fig. 1I–K). Collectively, these results demonstrated distinct contribution of the SHF-progenitor derived cells in the trunk of Ao and PA.

2.2. Identification of two waves of SHF progenitor-derived cells with differential preference for the Ao and PA

The distinct patterns of *Mef2c-AHF*+ in the trunk of Ao and PA suggests of unequal distribution of their progenitors to these two great arteries prior OFT septation. We next investigated this possibility.

Inducible *Mef2c-AHF-CreERT2; Rosa26*-mTmG (*Mef2c-AHF-CreERT2; mTmG*) mouse line was generated for temporo-spatial tracing of the *Mef2c-AHF* + cell lineage during OFT development. As indicated in Fig. 2A, tamoxifen was administrated to *Mef2c-AHF-CreERT2; mTmG* embryos at E7.5, E8.5, E9.5, E10.5 and E11.5, respectively (by intraperitoneal injection to pregnant female mice for one dose), and these embryos were dissected at E12.5 when OFT septation into Ao and PA was just complete, for lineage analysis in the two great arteries. The results revealed that upon *Mef2c-AHF* +progenitors were labeled at E7.5, a majority of their derivatives contributed to the Ao (Fig. 2B and C). However, those labeled after E7.5 (from E8.5 to E11.5) made their favorite route to the PA (Fig. 2B and C). These data demonstrated two waves of *Mef2c-AHF* +progenitors and their derivatives with differential preference to the Ao and PA. The first wave of the progenitors at E7.5 was preferentially destined to the Ao and the second wave of cells (from E8.5 to E11.5) made its favorite path to the PA.

Next, we performed detailed study to understand the dynamic contribution of these two waves of cells to the great arteries. For the first wave of cells, we labeled them at E7.5 and analyzed their fate at E10.5,

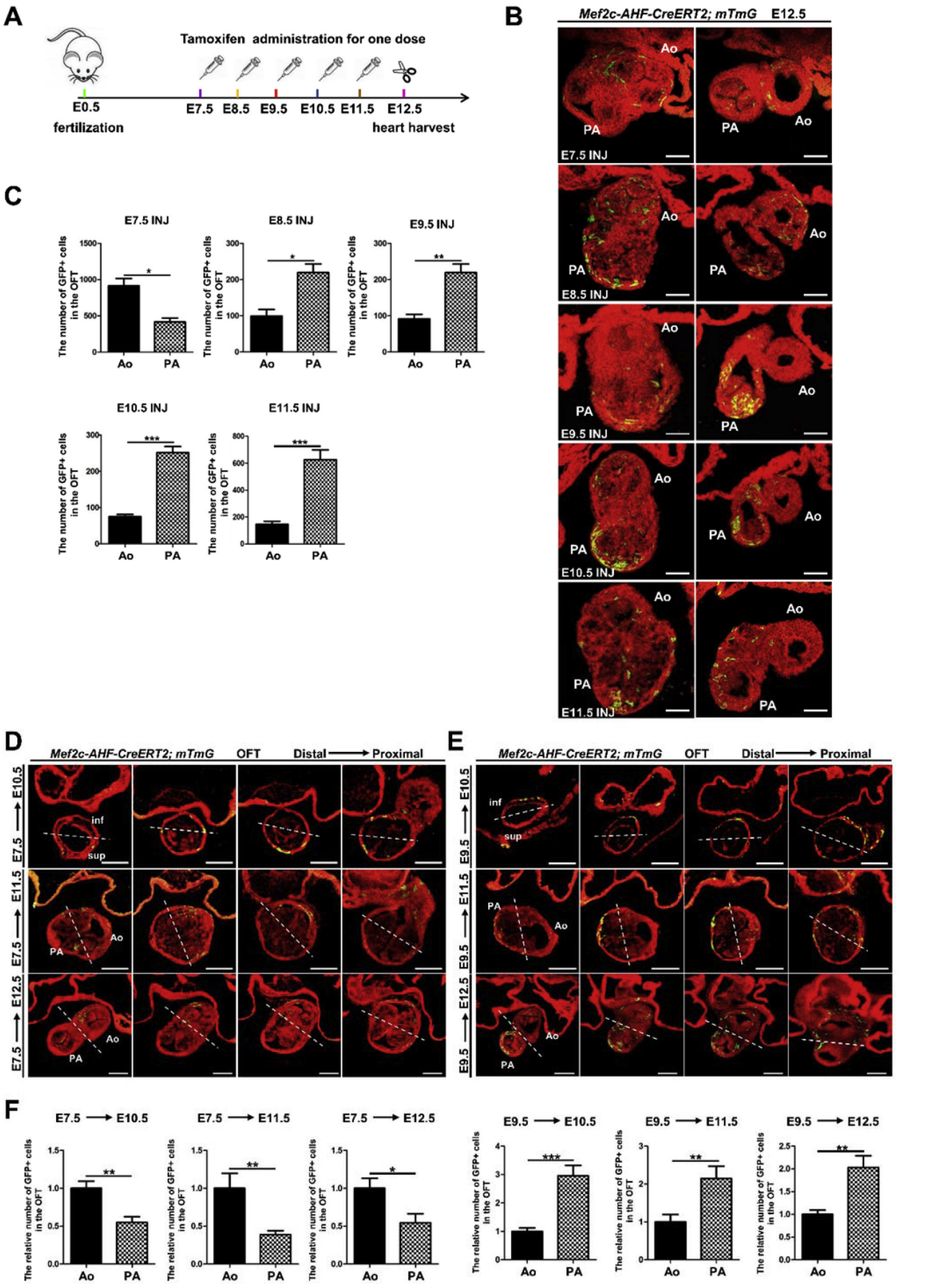

(caption on next page)

Fig. 2. Identification of two waves of *Mef2c-AHF* +cells with differential preference to the Ao and PA. **(A)** Time points of tamoxifen administration and OFT harvest. **(B)** Temporo-spatial analysis of the *Mef2c-AHF* +cells (in green) at single-cell resolution. Scale bars, 75 μm. **(C)** Quantitative analysis of the GFP + cells in each group for minimal 10 independent samples. **(D** and **E)** Serial sections of the OFT from distal to proximal part for lineage tracing of the *Mef2c-AHF* +cells (in green) at indicated time points. Dotted lines represented the prospective septation lines of the OFT. Scale bars, 100 μm. INJ, injection of tamoxifen; inf, inferior region; sup, superior region. **(F)** Quantitative analysis of the GFP + cells in each group for minimal 11 independent samples.

E11.5 and E12.5, respectively. We observed that the labeled *Mef2c-AHF* +cells tended to appear in the superior wall of the OFT at E10.5 and thereafter were shown predominantly in myocardium of the Ao (Fig. 2D). The second wave of cells was labeled at E9.5 and its destiny was followed up at the time points as for the first wave of cells (E10.5, E11.5 and E12.5). We found a preferential localization of these cells in the inferior wall of the OFT at E10.5, a complementary pattern to those labeled at E7.5 (Fig. 2E and F). Afterwards, the destiny of these cells was primarily identified in myocardium of the PA (Fig. 2E and F).

Taken together, results from these genetic lineage tracing studies identified two waves of *Mef2c-AHF* +progenitors and their derivatives with differential preference to the Ao and PA.

2.3. PDK1 as a pivotal regulator of the second wave of SHF progenitor-derived cells

Our previous study has demonstrated the crucial role of PTEN-PDK1-Akt signaling pathway in regulating the SHF progenitor expansion involved in the development of the OFT and the right ventricle (Luo et al., 2015). PDK1 is an upstream kinase that robustly activates Akt proteins, which controls cell and organ growth and function (Mora et al., 2004). To test whether PDK1 regulates the *Mef2c-AHF* + progenitors and their derivative cells implicated in Ao and PA development, we deleted *Pdk1* in these cells to obtain *Pdk1*$^{F/F}$; *Mef2c-AHF-Cre* mice (Lawlor et al., 2002; Zhao et al., 2014).

Morphological examination revealed that the *Pdk1* mutant embryos were indistinguishable from the controls at E9.5 (Figure S1A). Quantitative analysis of the OFT diameter (width) and length showed no significant difference between control and *Pdk1* mutant embryos (Figure S1B). However, study of the OFT from E10.5 embryos unveiled profoundly reduced size of both the proximal and distal OFT diameter in *Pdk1* mutant hearts, although the length of the OFTs is comparable between the two groups (Fig. 3A and B). At E11.5, the difference of OFT width between *Pdk1* mutants and controls was more apparent, particularly in the distal part (Fig. 3C and D).

These results suggested that the development of the second wave of *Mef2c-AHF* +progenitors and their derivatives might be impaired in the *Pdk1* mutants. To test this, we investigated the Isl1-and Mef2c-double positive cells (representing the SHF progenitors and their derivatives) in the OFT of E9.5 mice and found remarkably decreased number in the *Pdk1* mutants compared to the controls (Fig. 3E and F). This change was further confirmed in the OFT of E10.5 mice (Fig. 3G). Therefore, deletion of *Pdk1* impeded the contribution of the second wave of *Mef2c-AHF* +progenitors and their derivatives to OFT.

In consistence with these results, the nascent PA of *Pdk1* mutants displayed substantially narrowed lumen compared with controls at E12.5 when OFT septation was complete (Fig. 4A and B). Quantitative analysis confirmed this defect and manifested normal Ao development in *Pdk1* mutants (Fig. 4C). Histological study of E13.5 embryos also displayed reduced size of PA but normal Ao in *Pdk1* mutants, which is maintained from E16.5 to birth (Fig. 4D–F).

Furthermore, we examined the lung development that is connected to the pulmonary arteries in the embryos. We found that the lung development was not affected in Pdk1 mutant mice (Supplemental Fig. S2).

3. Discussion

In this study, we illuminated the assignment of the SHF progenitors and their derivatives to the two great arteries, the Ao and PA during OFT septation. Two waves of SHF-originated cells have been identified and their favorite migratory paths were elucidated. Meanwhile, we have defined PDK1 as a critical regulator of the second wave of cells.

Ten years ago, Dr. Buckingham and colleagues used two artificial transgenic mouse *LacZ* reporter lines (*y96-Myf5-nlacZ-16* and *A17-Myf5-nlacZ-T55*) to study the myocardial differences at the base of the great arteries and defined a prefigured characteristic of progenitor cell populations in the anterior heart field at E9.5 (Bajolle et al., 2006, 2008). This work for the first time clarified the distinct cellular origins for the bases of the two great arteries.

Compared to their work, our study has uncovered novel distinct properties of the SHF progenitors and their derivatives in the development of Ao and PA. First, the mouse tools for this study are inducible fluorescence reporter system that can follow up cell lineage at single-cell resolution in a temporo-spatial manner, which provides the dynamic position information of labeled cells more precisely than *LacZ* reporter system. Second, we have identified two waves of cell population, one at E7.5 and the other from E8.5 till E11.5 that make preferential contribution to the development of Ao and PA, respectively. Third, we figured out PDK1 as a pivotal protein in regulating the second wave of cells in the process of PA formation.

Our recent work reveals that the PTEN-PDK1-Akt signaling controls the SHF progenitor proliferation and differentiation through studying the *Pten* deletion mice (Luo et al., 2015). Here we dissected a more specific role of PDK1 in regulating a sub-population of the SHF progenitors involved in PA development.

In the future, it will be interesting and necessary to characterize the two waves of SHF progenitor-derived cells using high-throughput single cell sequencing technology to better understand the underlying regulatory mechanisms.

One disadvantage of our lineage tracing system (*Mef2c-AHF-CreERT2*) is that it cannot efficiently delete a gene because sufficient ablation of a gene needs high-dose tamoxifen, which is toxic to embryos leading to abortion.

This study help understand the pathogenesis of pulmonary stenosis (PS) that occurs either as a component of complex CHD (such as Tetrology of Fallot) or as an isolated anomaly. Our results suggest that abnormal development of the second wave of cells or impaired PDK1 signaling could be the causes for PS. Manipulation of these regulatory mechanisms might be applied for therapeutics of PA.

4. Materials and methods

4.1. Mice

The previously described mouse strains used in this study included *Mef2c-AHF-Cre* mice (Luo et al., 2015), *ROSA26*-mTmG mice (Xiao et al., 2017) and *Pdk1* floxed mice (Zhao et al., 2014). Generation of *Mef2c-AHF-CreERT2* mice will be described elsewhere. All mouse lines were maintained in a C57BL/6J genetic background. The experimental animal facility has been accredited by Association for Assessment and Accreditation of Laboratory Animal Care International (AAALAC) and the Institutional Animal Care and Use Committee (IACUC) of Model Animal Research Center of Nanjing University approved all animal protocols used in this study. Mice were housed in accordance with the regulations on mouse welfare and ethics of Nanjing University in groups with 12-h dark-light cycles and had free access to food and water.

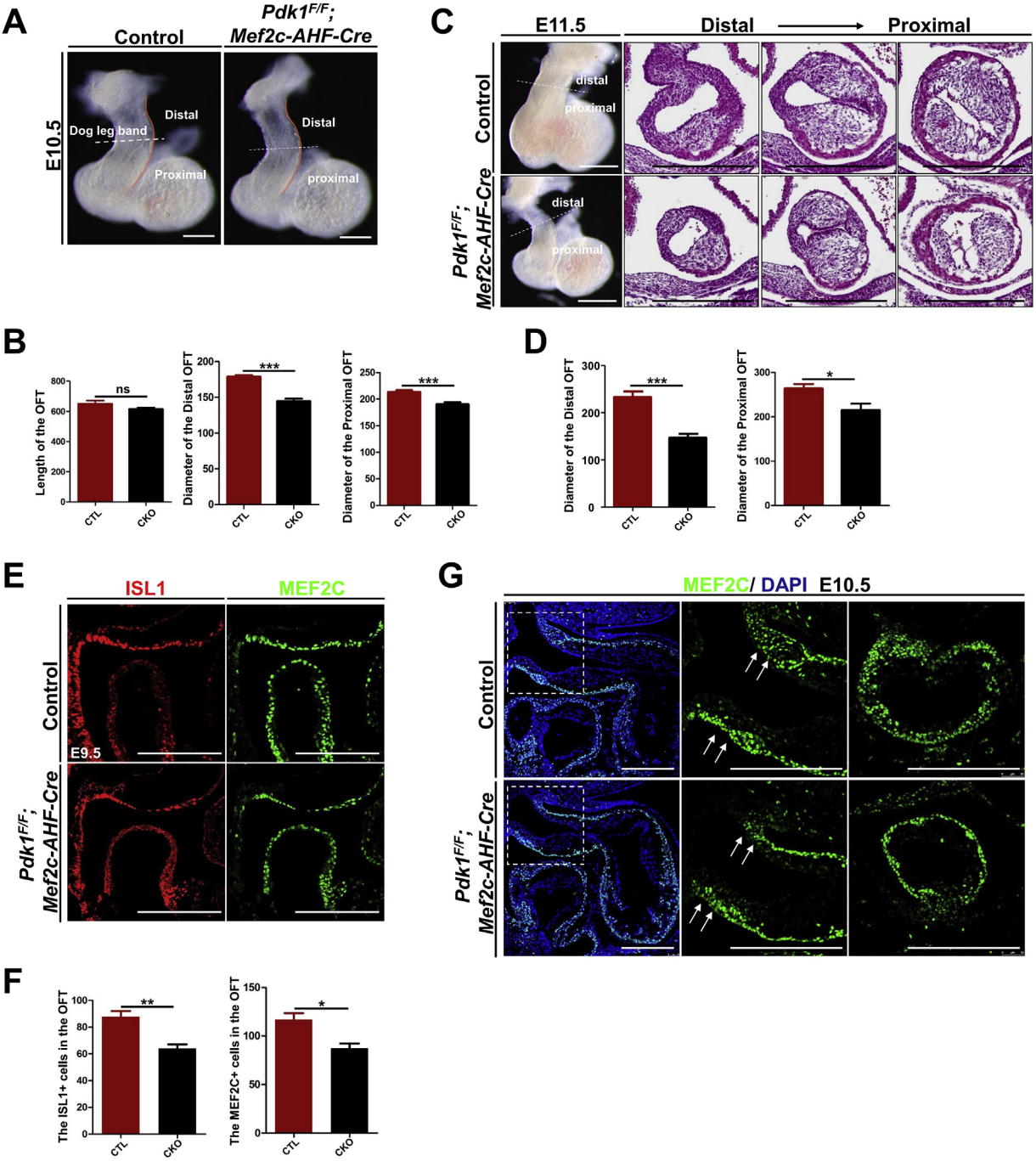

Fig. 3. Ablation of *Pdk1* resulted in defective contribution of the second wave of *Mef2c-AHF* +progenitors and their derivatives to OFT. **(A)** Gross analysis of the E10.5 OFT. Scale bars, 150 μm. **(B)** Quantitative analysis of the OFT length and the diameter (width) of distal and proximal OFT at E10.5, respectively (N = 5). *Pdk1* mutant mice showed significantly reduced diameter of OFT. **(C)** Gross and histological analysis of E11.5 OFTs. Scale bars, 200 μm. **(D)** Quantitative analysis of the diameter of distal and proximal OFT at E11.5 (N = 5). **(E and F)** IF staining of E9.5 OFT sections for ISL1 (red) and MEF2C (green). The cell number of ISL1 and MEF2C was quantitated (N = 5). Scale bars, 250 μm. **(G)** IF staining of E10.5 OFT sections for MEF2C (green). DAPI stained the nuclei (in blue). The distal and proximal parts of the single-tubular OFT were separated by a characteristic dog-leg bend. Scale bars, 150 μm. CTL: $Pdk1^{F/F}$ or $Pdk1^{F/+}$. CKO: $Pdk1^{F/F}$; *Mef2c-AHF-Cre*.

4.2. Histological analysis

For paraffin sections, mouse embryos or hearts were dissected and fixed in 4% paraformaldehyde on ice, then dehydrated in alcohol gradient, embedded in paraffin and sectioned. Histological sections were stained with hematoxylin and eosin (H&E) and immunofluorescence (IF) staining assays. For frozen sections, samples were fixed in 4% paraformaldehyde for no more than 2 h. After fixation, the embryos were rinsed in 1xPBS and incubated in 30% sucrose at 4 °C to sink gradually. The embryos were then embedded in OCT medium, quickly frozen in liquid nitrogen and stored at −80 °C.

4.3. Immunofluorescence

IF staining was performed on paraffin or frozen sections. For the paraffin sections, antigen retrieval was performed for 30 mins in boiled sodium citrate buffer. Slides were blocked in 10% goat serum for 1 h at room temperature (RT), washed 3 times in 1xPBS for 5 mins each and

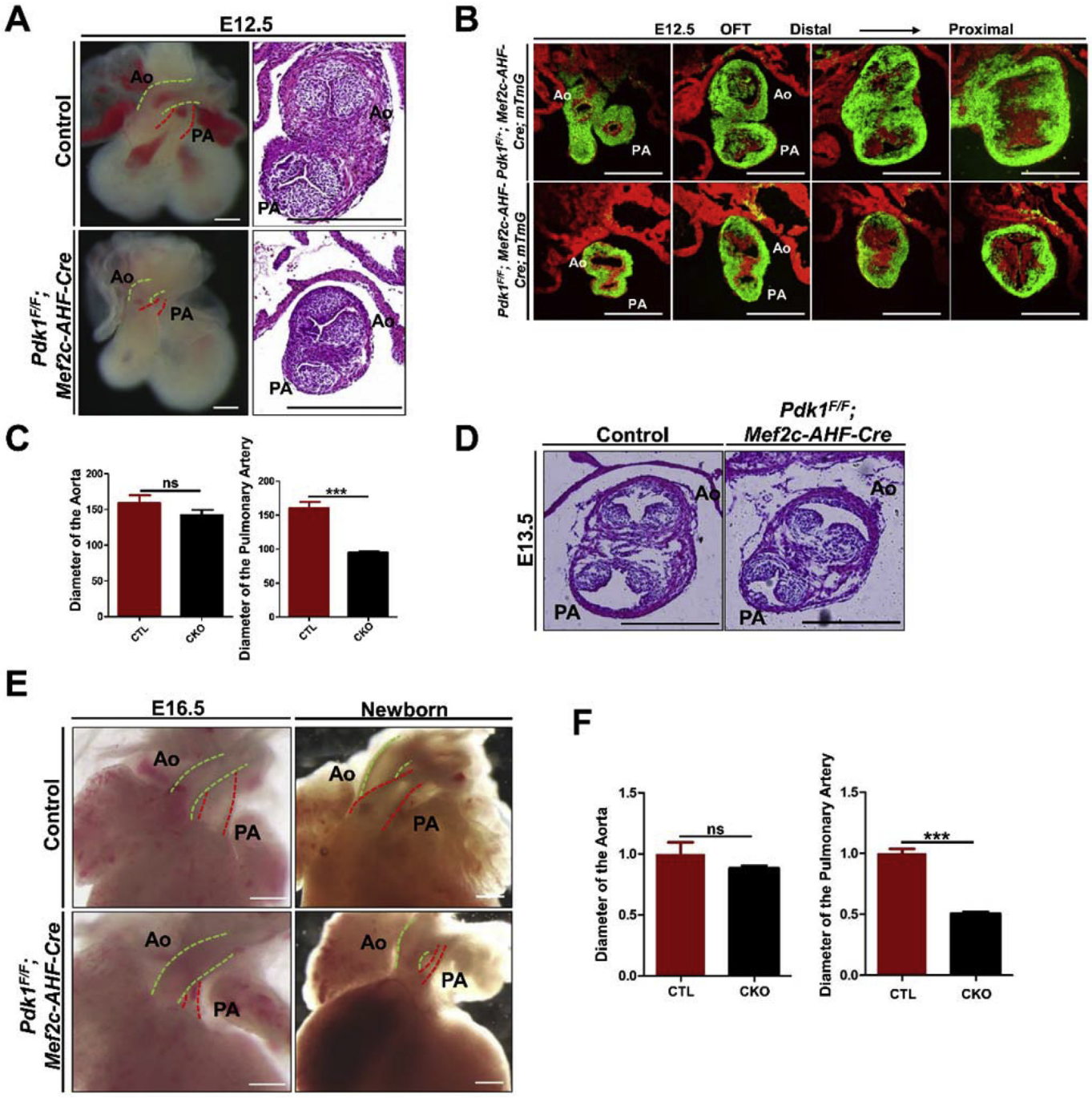

Fig. 4. PDK1 in the SHF-derived cells regulated the pulmonary artery formation and development. (A) Gross and histological analysis of the E12.5 OFTs. Scale bars, 250 μm. **(B)** Lineage tracing of the *Mef2c-AHF* +cells in the OFTs at E12.5. Compared with controls, the PA was poorly developed in *Pdk1* mutant mice. Scale bars, 200 μm. **(C)** Quantitative analysis of the diameter of distal and proximal OFT at E12.5 (N = 5). *Pdk1* mutant mice showed significantly reduced distal OFT diameter. **(D)** Histological analysis of the Ao and PA at E13.5. Scale bars, 350 μm. **(E)** Gross analysis of the great arteries at E16.5 and in newborn mice, respectively. Pulmonary stenosis (PS) was apparent in *Pdk1* knockout mouse (*$Pdk1^{F/F}$; Mef2c-AHF-Cre*). **(F)** Quantification of the diameter of Ao and PA in E16.5 mice. Scale bars, 250 μm. CTL: *$Pdk1^{F/F}$* or *$Pdk1^{F/+}$*. CKO: *$Pdk1^{F/F}$; Mef2c-AHF-Cre*.

incubated with primary antibodies overnight at 4 °C. The following day, sections were washed in 1xPBS three times (5 mins each wash) and incubated with secondary antibodies for 2 hs at RT. Then slides were rinsed three times (5 mins each wash) in 1XPBS and mounted in 50% triglyceride. For frozen sections, there was no need to do antigen retrieval. IF images were captured with, a Leica SP5 confocal laser microscope. The following antibodies were used for immunofluorescence staining: ISL1 (Developmental Studies Hybridoma Bank, 40.2D6), MEF2C (Cell Signaling Technology, #5030) and DAPI (Sangon #D6584).

4.4. Tamoxinfen injection

Tamoxifen administration was carried out via intraperitoneal injection to activate Cre recombination activity. Dose of Tamoxifen was related to the gestation age and body weight of pregnant mice. Tamoxifen was prepared as a 5 μg/μl stock solution in 90% maize oil with 10% ethanol (Ethanol was used to dissolve Tamoxifen, worked as a mediator between maize oil and Tamoxifen). Treatment of pregnant mice with 37.5 μg/g (Tamoxifen/body weight) was carried out at E7.5, while

Table 1
Key resources table.

Reagent or resource	Source	Identifier
Antibodies		
ISL1	Developmental Studies Hybridoma Bank	Cat# 40.2D6
MEF2C	CST	Cat# 5030
PDK1	Abcam	Cat# ab52893
KI67	Abcam	Cat# ab15580
PHH3	CST	Cat# 9701
cTnT	Life	Cat# MA5-12960
Alexa Fluor 488-AffiniPure Goat Anti-Rabbit IgG (H + L)	Jackson ImmunoResearch Labs	Cat# 111-545-144
Alexa Fluor 488-AffiniPure Goat Anti-Mouse IgG (H + L)	Jackson ImmunoResearch Labs	Cat# 115-545-166
Cy3-AffiniPure Goat Anti-Rabbit IgG (H + L)	Jackson ImmunoResearch Labs	Cat# 111-165-144
Cy3-AffiniPure Goat Anti-Mouse IgG (H + L)	Jackson ImmunoResearch Labs	Cat# 115-165-166
Chemicals, Peptides, and Recombinant Proteins		
DAPI	Santa Cruz	Cat# sc-3598
Sheep serum	BOSTER	Cat# AR0009
Tamoxifen	Sigma-Aldrich	Cat# T5648-1G
Experimental Models: Organisms/Strains		
Mef2c-AHF-Cre mice (STOCK Tg(Mef2c-Cre)1Blk/Mmnc)	Purchased from MMRRC	030261-UNC
Mef2c-AHF-CreERT2 mice	This study	N/A
*ROSA*26-mTmG mice (Gt(ROSA)26Sor$^{tm4(ACTB-tdTomato,-EGFP)Luo}$)	Purchased from Jackson Laboratory	Stock No. 007676
Pdk1 floxed mice	Gift from Dario Alessi	N/A
Oligonucleotides		
Oligonucleotides for genotyping *Pdk1* Forward: TGTGCTTGGTGGATATTGAT Reverse: AAGGAGGAGAGGAGGAATGT	This paper	N/A
Oligonucleotides for genotyping mTmG Wildtype Forward: CTCTGCTGCCTCCTGGCTTCT Wildtype Reverse: CGAGGCGGATCACAAGCAATA Mutant: TCAATGGGCGGGGGTCGTT	This paper	N/A
Software and Algorithms		
Leica confocal software	http://softadvice.informer.com/Leica_Confocal_Software.html	N/A
GraphPad Prism 5	https://www.graphpad.com/scientificsoftware/prism/	N/A
Adobe Photoshop CS6	https://creative.adobe.com/products/dow	N/A
Zeiss confocal software	https://www.zeiss.com/microscopy/int/products/microscope-software/zen.html	N/A

150 μg/g for other days. Embryos were harvested at specific date according to the experimental requirements.

4.5. Acquisition and processing of images

IF images were acquired with Leica (SP5) and Zeiss (LSM880) confocal softwares. Images were prepared using Photoshop CS6 (Adobe). Any changes to brightness and contrast were applied equally across the entire image.

4.6. Measurement and statistical analysis

The OFT length and diameter were measured using ImageJ software. For cell clonal experiments, all data were obtained on serial sections from ten or more embryos as indicated in each figure legend. The results were presented as the mean ± SEM values. Statistical calculations were performed using unpaired 2-tailed Student t-tests with GraphPad Prism5 software. A value of $P < 0.05$(*) was considered as statistically significant, and $P < 0.01$(**) or $P < 0.005$(***) was accepted as statistically very significant.

Please refer to the KRT Table 1.

Conflicts of interest

The authors declare no competing or financial interests.

Author contributions

H.J., H.W., J.L., M.X., Z.Q., M.X., J.Z. and Q.F. conducted the experiments, S. Y. maintained mouse breeding, J. X. and B. X. provided financial support, H.J., H. W. and Z.Y. designed the experiments and analyze the data. H. J. and Z. Y. wrote the paper.

Acknowledgements

The authors thank Dr. Dario Alessi for providing the *Pdk1* floxed (*Pdk*$^{F/F}$) mice (Lawlor et al., 2002). This work was supported by grants from the National Natural Science Foundation of China (31571490, 81741003, 91854111 and 91519312) to Zhongzhou Yang and by grants from the National Key Basic Research Program of China (2012CB966600 and 2011CB943904) and the State Key Laboratory of Genetic Engineering of Fudan University (SKLGE-1604) to Zhongzhou Yang.

Appendix A. Supplementary data

Supplementary data to this article can be found online at https://doi.org/10.1016/j.ydbio.2019.03.019.

References

Bajolle, F., Zaffran, S., Kelly, R.G., Hadchouel, J., Bonnet, D., Brown, N.A., Buckingham, M.E., 2006. Rotation of the myocardial wall of the outflow tract is implicated in the normal positioning of the great arteries. Circ. Res. 98, 421–428.
Bajolle, F., Zaffran, S., Meilhac, S.M., Dandonneau, M., Chang, T., Kelly, R.G., Buckingham, M.E., 2008. Myocardium at the base of the aorta and pulmonary trunk is prefigured in the outflow tract of the heart and in subdomains of the second heart field. Dev. Biol. 313, 25–34.
Bruneau, B.G., 2008. The developmental genetics of congenital heart disease. Nature 451, 943–948.
Buckingham, M., Meilhac, S., Zaffran, S., 2005. Building the mammalian heart from two sources of myocardial cells. Nat. Rev. Genet. 6, 826–835.
Dyer, L.A., Kirby, M.L., 2009. The role of secondary heart field in cardiac development. Dev. Biol. 336, 137–144.

Fahed, A.C., Gelb, B.D., Seidman, J.G., Seidman, C.E., 2013. Genetics of congenital heart disease: the glass half empty. Circ. Res. 112, 707–720.
Francou, A., Saint-Michel, E., Mesbah, K., Theveniau-Ruissy, M., Rana, M.S., Christoffels, V.M., Kelly, R.G., 2013. Second heart field cardiac progenitor cells in the early mouse embryo. Biochim. Biophys. Acta 1833, 795–798.
Kirby, M.L., Gale, T.F., Stewart, D.E., 1983. Neural crest cells contribute to normal aorticopulmonary septation. Science 220, 1059–1061.
Lawlor, M.A., Mora, A., Ashby, P.R., Williams, M.R., Murray-Tait, V., Malone, L., Prescott, A.R., Lucocq, J.M., Alessi, D.R., 2002. Essential role of PDK1 in regulating cell size and development in mice. EMBO J. 21, 3728–3738.
Luo, W., Zhao, X., Jin, H., Tao, L., Zhu, J., Wang, H., Hemmings, B.A., Yang, Z., 2015. Akt1 signaling coordinates BMP signaling and beta-catenin activity to regulate second heart field progenitor development. Development 142, 732–742.
Meilhac, S.M., Lescroart, F., Blanpain, C., Buckingham, M.E., 2015. Cardiac cell lineages that form the heart. Cold Spring Harbor Perspect. Med. 5, a026344.
Mora, A., Komander, D., van Aalten, D.M., Alessi, D.R., 2004. PDK1, the master regulator of AGC kinase signal transduction. Semin. Cell Dev. Biol. 15, 161–170.
Neeb, Z., Lajiness, J.D., Bolanis, E., Conway, S.J., 2013. Cardiac outflow tract anomalies. Wiley Interdiscip. Rev. Develop. Biol. 2, 499–530.
Plein, A., Calmont, A., Fantin, A., Denti, L., Anderson, N.A., Scambler, P.J., Ruhrberg, C., 2015. Neural crest-derived SEMA3C activates endothelial NRP1 for cardiac outflow tract septation. J. Clin. Investig. 125, 2661–2676.
Sawada, H., Rateri, D.L., Moorleghen, J.J., Majesky, M.W., Daugherty, A., 2017. Smooth muscle cells derived from second heart field and cardiac neural crest reside in spatially distinct domains in the media of the ascending aorta-brief report. Arterioscler. Thromb. Vasc. Biol. 37, 1722–1726.
Srivastava, D., 2006. Making or breaking the heart: from lineage determination to morphogenesis. Cell 126, 1037–1048.
Van den Hoff, M.J., Moorman, A.F., Ruijter, J.M., Lamers, W.H., Bennington, R.W., Markwald, R.R., Wessels, A., 1999. Myocardialization of the cardiac outflow tract. Dev. Biol. 212, 477–490.
Verzi, M.P., McCulley, D.J., De Val, S., Dodou, E., Black, B.L., 2005. The right ventricle, outflow tract, and ventricular septum comprise a restricted expression domain within the secondary/anterior heart field. Dev. Biol. 287, 134–145.
Waldo, K.L., Hutson, M.R., Ward, C.C., Zdanowicz, M., Stadt, H.A., Kumiski, D., Abu-Issa, R., Kirby, M.L., 2005. Secondary heart field contributes myocardium and smooth muscle to the arterial pole of the developing heart. Dev. Biol. 281, 78–90.
Webb, S., Qayyum, S.R., Anderson, R.H., Lamers, W.H., Richardson, M.K., 2003. Septation and separation within the outflow tract of the developing heart. J. Anat. 202, 327–342.
Xiao, Q., Zhang, G., Wang, H., Chen, L., Lu, S., Pan, D., Liu, G., Yang, Z., 2017. A p53-based genetic tracing system to follow postnatal cardiomyocyte expansion in heart regeneration. Development 144, 580–589.
Zeigler, V.L., 2008. Congenital heart disease and genetics. Crit. Care Nurs. Clin. 20, 159–169 (v).
Zhao, X., Lu, S., Nie, J., Hu, X., Luo, W., Wu, X., Liu, H., Feng, Q., Chang, Z., Liu, Y., et al., 2014. Phosphoinositide-dependent kinase 1 and mTORC2 synergistically maintain postnatal heart growth and heart function in mice. Mol. Cell Biol. 34, 1966–1975.